Proceedings of the 46th International School and Conference on the Physics of Semiconductors "Jaszowiec" 2017, Szczyrk

Photoluminescence Studies of Excitonic Complexes in Atomically Thin $Mo(S_ySe_{1-y})_2$ Alloys

J. Jadczak*

Department of Experimental Physics, Wrocław University of Science and Technology, Wrocław, Poland

Transition metal dichalcogenides show new emergent properties at monolayer thickness, notably strong Coulomb and electron–phonon interactions enable new insight into physics of many body effects. Here, we report photoluminescence and reflectivity contrast measurements of excitons (X) and trions (T) and the Raman spectra of phonons in monolayers of $Mo(S_ySe_{1-y})_2$ alloys with sulfur mole content from $y = 0$ up to $y = 1$. Binary $MoSe_2$ and ternary $Mo(S_ySe_{2-y})$ alloys exhibit contrasting behavior in the temperature evolution of excitons and trions photoluminescence intensity from $T = 7 - 295$ K. In $MoSe_2$ a trion dominates photoluminescence spectra at low temperatures but exciton dominates photoluminescence at higher temperature. In contrast, in ternary $Mo(S_ySe_{1-y})_2$ alloys and MoS_2 trions dominate photoluminescence spectra at all measured temperatures, with the trion to exciton photoluminescence intensity ratio increasing with sulfur content. We attribute the strong increase of the trion photoluminescence intensity in $Mo(S_ySe_{1-y})_2$ monolayers with increase of sulfur mole content to the significant increase of the two-dimensional electron gas concentration and also to the strong exciton-trion coupling mediated by an optical phonon. We also demonstrate that increasing sulfur content in $Mo(S_ySe_{1-y})_2$ alloys stabilizes total photoluminescence intensity at high temperature.

DOI: 10.12693/APhysPolA.132.307

PACS/topics: Transition metal dichalcogenides monolayers, exciton, trion, phonon

1. Introduction

There is currently significant interest in two-dimensional semiconductors based on transition metal dichalcogenides (TMDCs), such as WSe_2, WS_2, $MoSe_2$, MoS_2, following the demonstration of the indirect-to-direct bandgap transition and strong spin and valley coupling in a single monolayer (ML) [1–10]. In MLs of TMDCs the bottom of the conduction band and the top of the valence band are located at the K points of two-dimensional (2D) hexagonal Brillouin zone. The strong spin–orbit coupling and lack of inversion symmetry lead to valley-contrasting strong spin splitting of valence and conduction bands [4–12]. The direct energy gap in the visible spectral range and the coupling of the spin and valley degree of freedom make TMDCs very promising for photonics and spintronic applications [3–21]. The confinement to a single layer and reduced dielectric screening lead to strong many body effects mediated by Coulomb interactions. In monolayers of TMDCs excitons, bound electron–hole pairs (X), exhibit very high binding energies of a few hundreds of meV [22–28]. In the presence of access carriers charged excitons, trions (T), consisting of two electrons and one hole, or two holes and one electrons are reported [29–32] in optical spectra of TMDCs MLs. In selenides, $MoSe_2$ and WSe_2 the photoluminescence intensity of a trion is high at low temperatures but rapidly disappear from the PL spectra with the increase of temperature [32].

We present detailed temperature dependent ($T = 7 - 295$ K) photoluminescence (PL) studies of excitons and trions in binary, $MoSe_2$ and MoS_2 ternary $Mo(S_ySe_{1-y})_2$ MLs with compositions $y = 0.1$, 0.2, 0.3, and 0.5. Additionally, we performed complementary measurements of reflectivity contrast (RC) and the Raman scattering spectra of all MLs. Binary $MoSe_2$ and ternary $Mo(S_ySe_{1-y})_2$ alloys exhibit very different temperature evolution of the exciton and trion PL intensity. In $MoSe_2$ trion dominates in PL spectra at low temperatures but strongly decreases in intensity with the increase of temperature range. In contrast, in PL spectra of ternary $Mo(S_ySe_{1-y})_2$ and binary MoS_2 MLs trions dominate in PL spectra at all measured temperatures ($T = 7 - 295$ K). Confinement to a single layer Coulomb and reduced dielectric screening yields also to strong binding energy of charged excitons in TMDCs [30–33]. In selenides $MoSe_2$ and WSe_2 binding energy of an additional electron or hole to a neutral exciton is equal to 30 meV and is comparable with energies of optical phonons [33–36] which leads to strong coupling of the exciton and trion by exchange of an optical phonon [37]. In $MoSe_2$ the A_1' optical phonon energy, 29.8 meV [33], resonances with the trion binding energy equal 30 meV [33]. In MoS_2 the A_1' phonon energy of 51 meV [33] strongly exceeds those in $MoSe_2$. For that reason incorporation of sulfur atoms into $MoSe_2$ host lattice results in significant increase of the A_1' phonon energy [36]. We found that the high temperature trion to exciton PL intensity ratio (I_T/I_X) increase with sulfur mole content. We relate this effect to the substantial increase of two-dimensional electron gas (2DEG) concentration and also to the increase of the exciton–trion coupling mediated by the A_1' optical phonon. We also demonstrate that increasing sulfur con-

*e-mail: joanna.jadczak@pwr.edu.pl

tent in $Mo(S_ySe_{1-y})_2$ alloys stabilizes high temperature total PL. With the temperature growth from 6 K to 295 K the total PL in $MoSe_2$ decreases about four orders of magnitude whereas in $MoS_{1.0}Se_{1.0}$ only about 5 times.

2. Samples and experiment

We studied MLs of binary $MoSe_2$ and MoS_2, and ternary $Mo(S_ySe_{1-y})_2$ alloys elaborated by mechanical exfoliation from single crystals on SiO_2(300 nm)/Si substrate. The thicknesses of the mono- to few-layer flakes were established using optical contrast, the Raman spectroscopy and subsequently by observation of efficient photoluminescence. Bulk mixed crystals were grown by chemical vapor transport technique (CVT). Prior to the crystal growth the powdered compounds of the series were prepared from the elements (Mo: 99.99%, S: 99.999%, Se: 99.995%) by reaction at 1000 °C for 10 days in evacuated quartz ampoules. The S and Se materials were added in such manner that the S content y changing relatively to the Se content increases from 0 to 0.5 with a content step size $\Delta y = 0.1$. The chemical transport was achieved with I_2 as a transport agent in the amount of about 5 mg/cm^3.

The samples were mounted on the cold-finger of a non-vibrating closed cycle cryostat, where temperature can be varied from 7 to 300 K. For temperature-dependent PL experiments a 532 nm line of a diode-pumped solid state laser was used for excitation. The laser beam was focused on the sample under normal incidence using a 50× high resolution, long distance microscope objective (NA = 0.65). The diameter of excitation spot was equal to ≈ 1.5 μm. The spectra were analyzed with a 0.5 m focal length spectrometer and a 600 lines/mm grating. A Peltier-cooled Si charge coupled device was used as a detector. The RC and Raman spectra were measured in the same setup. In RC experiments a filament lamp was used as a light source. The polarization-resolved Raman scattering measurements were performed at room temperature in backscattering geometry with a 2400 groves/mm grating. The Raman signal was excited with σ^+ circularly polarized light and detected separately in σ^+ and σ^- polarizations.

3. Results and discussion

Figure 1 shows the evolution of the unpolarized Raman spectra of the $Mo(S_ySe_{1-y})_2$ monolayers measured at $T = 295$ K with concentration of sulfur allowing for the determination of phonon energy. For the binary $MoSe_2$, the frequencies of the first order Raman lines are equal to 240.6 cm^{-1} and 286 cm^{-1}. They are assigned to the out-of-plane A_1' and in-plane E_2' modes, respectively. As the composition y slightly increases, we can identify in the Raman spectra additional features in the range 200–280 cm^{-1}. The presence of a sulfur atom in the host lattice of $MoSe_2$ induces vibrations with out of plane weight in the vicinity of A_1' mode, resulting in characteristic splitting into two branches denoted as A_1' and A^*. The splitting is directly related to the different distribution of the chalcogenide atoms within the $Mo(S_ySe_{1-y})_2$ layers. As it is seen in Fig. 1, the A_1' (Se–Se) and A^* (Se–S) phonons evolve in a different manner as a function increasing S content y. Based on their intensities, we have divided them into two groups [33–36]. The first group, at lower frequencies, corresponds to the Se–Se configuration, whereas the second group at higher frequencies is likely related to the Se–S vibration [33–36]. Among mixed Se–S branch, we can identify at least three components, shifting to higher frequency upon increasing y. They are well resolved for $0.1 < y < 0.2$, when the $2Se_2 + 1SeS$, $2Se_2 + 1S_2$ or $1Se_2 + 2SeS$ arrangements are the most probable [33–36]. By contrast, Se–Se branch shifts to lower frequency. In bulk alloys, studied in our recent papers, this branch disappears from the Raman spectra when the sulfur content exceeds $y = 0.5$ [36].

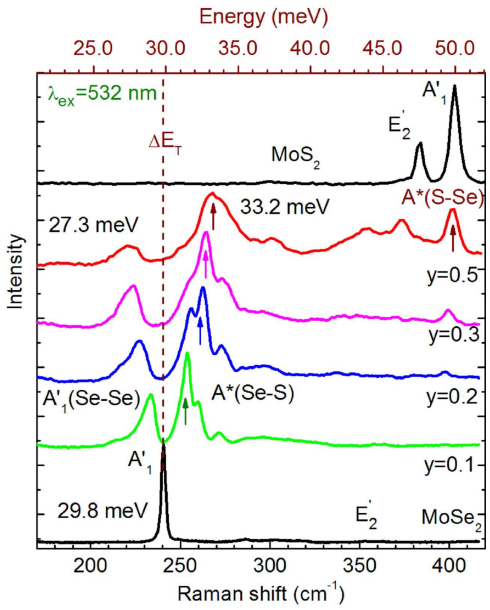

Fig. 1. The Raman spectra of all studied MLs recorded at $T = 300$ K.

Figure 2 presents examples of comparative RC and PL spectra of the studied MLs for $MoSe_2$, $Mo(S_{0.3}Se_{0.7})_2$, $Mo(S_{0.5}Se_{0.5})_2$ and MoS_2 at two temperatures $T = 10$ K and $T = 120$ K. In PL experiments the laser excitation power is relatively low ($P = 100$ μW) to avoid heating of the ML. At low temperature ($T = 10$ K) PL and RC spectra two distinct transitions, corresponding to the exciton and trion are recorded. Their energy positions are in a good agreement with the previous reports [29–32]. In PL spectra of MoS_2 an additional line (denoted as L, see also Fig. 3) is detected in the lower energy sector. The nature of this line is still under debate [1, 3] and is beyond the scope of this work. In PL spectra of all studied MLs at $T = 10$ K the PL intensity of the trion exceeds this of the exciton. Contrary to the PL spectrum, in the RC spectrum of $MoSe_2$ and $Mo(S_{0.3}Se_{0.7})_2$ the exciton resonance is stronger than this of the trion. In RC spectra

of $Mo(S_{0.5}Se_{0.5})_2$, the trion and exciton resonances are comparable and only in binary MoS_2 the trion resonance is stronger than that of exciton. The reason is that the strength of optical amplitude of the exciton and trion resonances in reflectivity are determined by respective density of states, whereas the PL intensity is contributed additionally by a state occupation factor. At low temperatures the excess carriers and photocreated electron–hole pairs thermalize into the same locations corresponding to minima of the potential fluctuations in the monolayer, leading to the increase of the probability of trion formation, which is observed as an increase of the trion emission relative to the exciton emission.

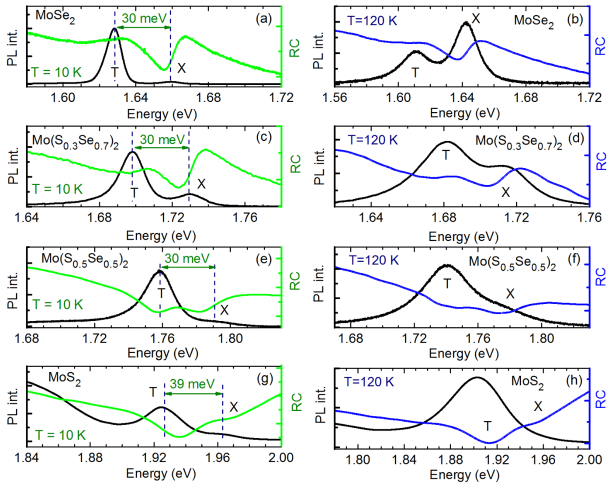

Fig. 2. Examples of comparative PL and RC spectra recorded at $T = 10$ K and $T = 120$ K for MLs of: (a) and (b) — $MoSe_2$, (c) and (d) — $Mo(S_{0.5}Se_{0.5})_2$, (e) and (f) — MoS_2.

The comparison of RC and PL spectra of $Mo(S_{0.1}Se_{0.9})_2$ and $Mo(S_{0.2}Se_{0.8})_2$ MLs are not presented as they exhibit the same relation as those of monolayers with low sulfur concentrations, $MoSe_2$ and $Mo(S_{0.3}Se_{0.7})_2$. The energy positions of the exciton and trion in monolayers of $Mo(S_ySe_{1-y})_2$ alloys shift to higher energies with the increase of the sulfur mole content with characteristic band gap bowing deviating from a strictly linear extrapolation between the binary bandgaps (not presented).

Figure 3 presents evolution of PL spectra as a function of temperature for all studied MLs. The corresponding spectrum for each temperature is normalized to one. The complementary Fig. 4 presents temperature dependence of the integrated PL intensity of excitons and trions, and the total integrated PL intensity for all monolayers, except binary MoS_2, as in this sample only the trion line is well resolved in the PL spectra at all measured temperatures. The common feature observed in PL spectra of all studied MLs is that at low temperatures the PL intensity of the trion exceeds this of the exciton, and that PL intensities of both lines decrease with increasing temperature but with substantially different rates for different MLs.

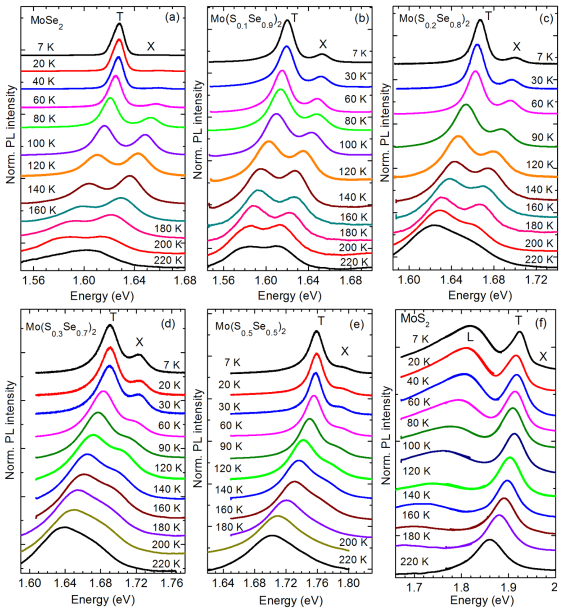

Fig. 3. The temperature evolution of PL spectra of: (a) $MoSe_2$, (b) $Mo(S_{0.1}Se_{0.9})_2$, (c) $Mo(S_{0.2}Se_{0.8})_2$, (d) $Mo(S_{0.3}Se_{0.7})_2$, (e) $Mo(S_{0.5}Se_{0.5})_2$, (f) MoS_2.

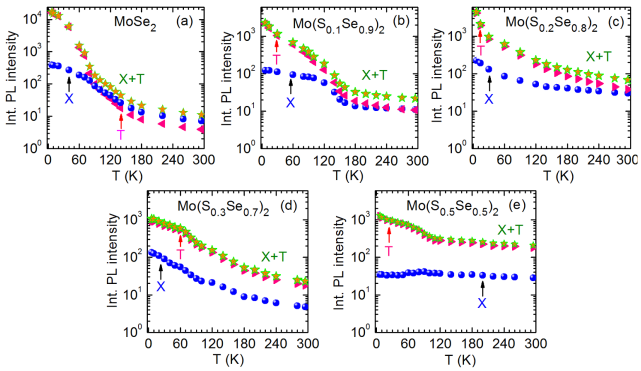

Fig. 4. The PL intensities of excitons and trions, and total PL intensity as a function of the temperature in: (a) $MoSe_2$, (b) $Mo(S_{0.1}Se_{0.9})_2$, (c) $Mo(S_{0.2}Se_{0.8})_2$, (d) $Mo(S_{0.3}Se_{0.7})_2$ and (e) $Mo(S_{0.5}Se_{0.5})_2$.

In binary $MoSe_2$ at $T = 7$ K the PL intensity of the trion is about 50 times stronger than that of the exciton. With temperature growth the exciton PL increases relatively to the trion PL, with the latter showing a dramatic reduction by about four orders of magnitude in the range from 7 K to 295 K. The PL intensity of X exceeds that of T at temperature above 140 K. The temperature evolution of PL spectra of ternary $Mo(S_ySe_{1-y})_2$ alloys exhibit gradual change from $MoSe_2$ with increase of the sulfur mole content. The most intriguing change is observed in temperature evolution of the trion to exciton PL intensities ratio (I_T/I_X) presented in Fig. 5. Two regimes of high and low temperature are distinguished. At low temperatures, below $T < 100$ K, the PL intensity of T is much higher than of X for all ternary samples but no evident correlation between I_T/I_X ratio and increase

of sulfur content is observed. At higher temperatures $T > 100$ K the I_T/I_X ratio in ternary $Mo(S_ySe_{1-y})_2$ MLs exceeds this of $MoSe_2$ and increases with the increase of the sulfur mole content. In all $Mo(S_ySe_{1-y})_2$ MLs we observe that the trion dominates emission at all measured temperatures. In binary MoS_2 the intensity only the trion line is distinguished in PL spectra at all measured temperatures. The exciton line is only hardly distinguished in PL spectra at low temperatures. The line L observed at low temperatures of PL spectra of MoS_2 is beyond the scope of this paper.

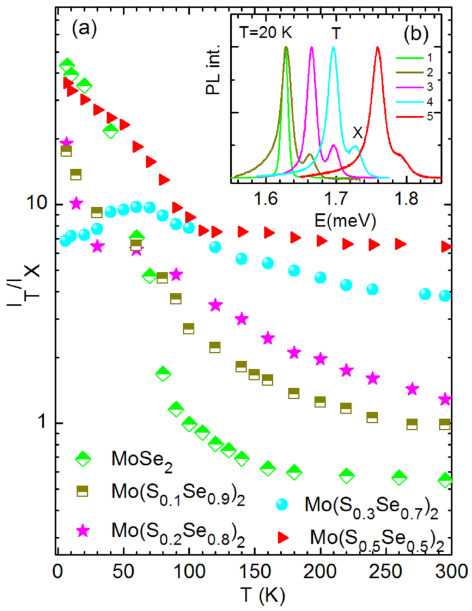

Fig. 5. The temperature dependence of the trion to exciton PL intensity ratio I_T/I_X in monolayers of $Mo(S_ySe_{1-y})_2$ alloys. In the inset the PL spectra of all studied samples recorded at $T = 20$ K are compared: (1) $MoSe_2$, (2) $Mo(S_{0.1}Se_{0.9})_2$, (3) $Mo(S_{0.2}Se_{0.8})_2$, (4) $Mo(S_{0.3}Se_{0.7})_2$, (5) $Mo(S_{0.5}Se_{0.5})_2$.

We attribute the observed increase in the trion emission in $Mo(S_ySe_{1-y})_2$ monolayers with the growth of the sulfur mole content to two effects: (1) the increase of the exciton–trion coupling mediated by optical phonon, (2) the growth of the 2D electron concentration. With the growth of the sulfur content the energy of the out of plane optical phonon A_1' increases (Fig. 1), which results in the increase of the exciton–trion coupling mediated by this phonon. Our interpretation is based on the recent work of Jones et al. [37], in which they demonstrated an efficient luminescence upconversion process from a trion to an exciton resonance in monolayer WSe_2, producing spontaneous anti-Stokes emission with an energy gain of 30 meV. They attributed this effect to a double resonant Raman scattering, where the incident and scattered photons are in resonance with the trion and the neutral exciton, respectively. Coupling between the trion and the exciton is realized by exchange of the out of plane optical phonon A_1'. In WSe_2 the optical phonon A_1' energy of 31 meV exceeds the trion binding energy equal to

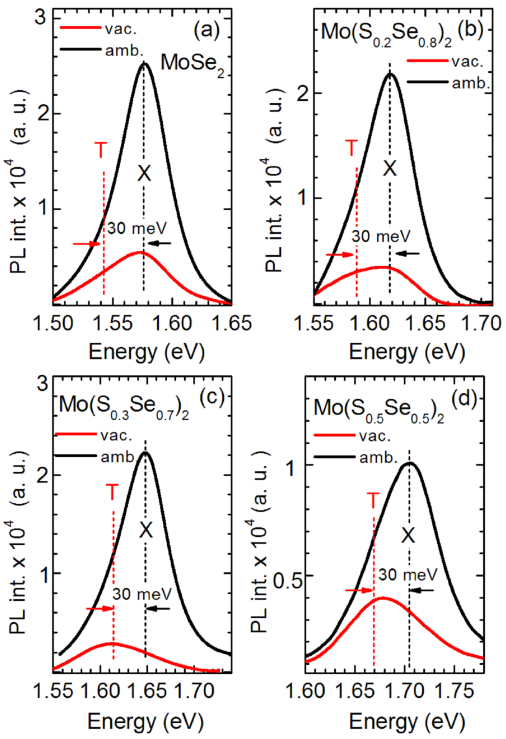

Fig. 6. The photoluminescence spectra recorded at $T = 295$ K in ambient and vacuum for (a) $MoSe_2$, (b) $Mo(S_{0.2}Se_{0.8})_2$, (c) $Mo(S_{0.3}Se_{0.7})_2$ and (d) $Mo(S_{0.5}Se_{0.5})_2$.

30 meV. In contrast, in $MoSe_2$ MLs, studied in this paper, the energy of A_1' optical phonon, equal to 29.8 meV, is slightly lower than the trion binding energy, equal to 30 meV, which results in weaker exciton–trion coupling, especially at higher temperatures, when excitons have additional kinetic energy proportional to kT. The increase of the A_1' optical phonon energy in $Mo(S_ySe_{1-y})_2$ alloys, for small sulfur content $y < 0.3$, results in almost linear increase of high temperature I_T/I_X ratio as a function of phonon energy E_{ph}, measured from the trion binding energy E_T (not shown). For the higher sulfur content $y \geq 0.3$ we observed abrupt increase of I_T/I_X ratio. We suggest that this abrupt increase is related to significant increase of 2DEG concentration in $Mo(S_ySe_{1-y})_2$ monolayers with increase of sulfur content. As reported in Refs. [3, 29] there is a substantial difference in the intrinsic two-dimensional electron gas concentration in $MoSe_2$ and MoS_2 monolayers in vacuum. In $MoSe_2$ MLs the background 2DEG concentration is of order 10^{10} cm^{-2} [29], whereas in MoS_2 MLs it is of order of 10^{12} cm^{-2} [3]. Hence one should expect the strong increase of the 2DEG concentration in $Mo(S_ySe_{1-y})_2$ MLs with the increase of the sulfur mole content.

The precise determination of the electron concentration requires conductivity measurements. As we do not have at abilities to conduct transport measurements on our monolayers we performed additional PL experiments demonstrating increase of 2DEG concentration with the

sulfur mole content. It is well established that under ambient conditions physisorbed O_2 and H_2O molecules deplete n-type materials such as MoS_2 and $MoSe_2$, much more than conventional electric field gating [38, 39]. In Fig. 6 we compare the PL spectra recorded at $T = 295$ K in ambient and vacuum conditions for different monolayers: (a) $MoSe_2$, (b) $Mo(S_{0.2}Se_{0.8})_2$, (c) $Mo(S_{0.3}Se_{0.7})_2$ and (d) $Mo(S_{0.5}Se_{0.5})_2$. The experiments are performed under the same conditions for all samples. As is clearly seen, under ambient condition for all monolayers the maximum of PL intensity is detected at the exciton, whereas in vacuum the maximum PL intensity shifts gradually from the exciton in $MoSe_2$ to the trion in $Mo(S_{0.5}Se_{0.5})_2$. This observation confirms qualitatively the increase of 2DEG concentration with the increase of sulfur mole content in $Mo(S_ySe_{1-y})_2$ MLs placed in vacuum. The shifts of the spectral weights of photoluminescence from the exciton to trion with increasing 2DEG concentration is well known from the study of $GaAs/Al_xGa_{1-x}As$ $CdTe/Cd_{1-x}Mg_xTe$ two-dimensional semiconductor structures [40–42].

4. Conclusion

In summary we report observation of robust trions in temperature dependent photoluminescence and reflectivity contrast studies of $Mo(S_ySe_{1-y})_2$ monolayers with sulfur mole content up to $y = 1$. We found significant difference in temperature evolution of the exciton and trion PL intensity of binary $MoSe_2$ and ternary $Mo(S_ySe_{1-y})_2$ monolayers. In $MoSe_2$ trion dominates in PL spectra at low temperatures but significantly decreases in intensity with increase of temperature. In contrast, in ternary $Mo(S_ySe_{1-y})_2$ alloys we observe robust trion emission, dominating PL spectra at all measured temperatures. Moreover, the high temperature trion to exciton PL intensity ratio increases with sulfur content. We attribute these observation to strong increase of the exciton–trion coupling and to strong increase of the two-dimensional electron gas concentration with increase of sulfur content.

Acknowledgments

This work was supported by the Polish NCN Grant No. 2013/09/B/ST3/02528, and the Polish-Taiwanese Joint Research OSTMED PL-TWII/5/2015. I thank Leszek Bryja for discussion, Joanna Kutrowska-Girzycka and Y.S. Huang for assistance in elaboration of the studied samples.

References

[1] K.F. Mak, C. Lee, J. Hone, J. Shan, T.F. Heinz, *Phys. Rev. Lett.* **105**, 136805 (2010).

[2] A. Splendiani, L. Sun, Y. Zhang, T. Li, J. Kim, C.Y. Chim, G. Galli, F. Wang, *Nano Lett.* **10**, 1271 (2010).

[3] B. Radisavljevic, A. Radenovic, J. Brivio, V. Giacometti, A. Kis, *Nat. Nanotechnol.* **6**, 147 (2011).

[4] Y. Zhang, T.R. Chang, B. Zhou, Y.T. Cui, H. Yan, Z. Liu, F. Schmitt, J. Lee, R. Moore, Y. Chen, H. Lin, H.T. Jeng, S.K. Mo, Z. Hussain, A. Bansil, Z.X. Shen, *Nat. Nanotechnol.* **9**, 111 (2014).

[5] E.S. Kadantsev, P. Hawrylak, *Solid State Commun.* **152**, 909 (2012).

[6] G.B. Liu, W.Y. Shan, Y. Yao, W. Yao, D. Xiao, *Phys. Rev. B* **88**, 085433 (2013).

[7] A. Kormanyos, G. Burkard, M. Gmitra, J. Fabian, V. Zólyomi, N.D. Drummond, V. Falko, *2D Mater.* **2**, 022001 (2015).

[8] H. Dery, Y. Song, *Phys. Rev. B* **92**, 125431 (2015).

[9] Q. Feng, J. Wang, H. Xing, J.F. Destino, M.M. Arik, Ch. Zhao, K. Kang, B. Blizzard, L. Zhang, P. Zhao, S. Huang, S. Yang, F.V. Bright, J. Cerne, H. Zeng, *Adv. Mater.* **26**, 2648 (2014).

[10] T. Cao, G. Wang, W. Han, H. Ye, Ch. Zhu, J. Shi, Q. Niu, P. Tan, E. Wang, B. Liu, J. Feng, *Nat. Commun.* **3**, 887 (2012).

[11] G. Sallen, L. Bouet, X. Marie, G. Wang, C.R. Zhu, W.P. Han, Y. Lu, P.H. Tan, T. Amand, B.L. Liu, B. Urbaszek, *Phys. Rev. B* **86**, 081301 (2012).

[12] G. Kioseoglou, A.T. Hanbicki, M. Currie, A.L. Friedman, D. Gunlycke, B. Jonker, *Appl. Phys. Lett.* **101**, 221907 (2012).

[13] X. Xu, D. Xiao, T.F. Heinz, W. Yao, *Nat. Phys.* **10**, 343 (2014).

[14] D. Xiao, G.B. Liu, W. Feng, X. Xu, W. Yao, *Phys. Rev. Lett.* **108**, 196802 (2012).

[15] T. Scrace, Y. Tsai, B. Barman, L. Scheidenback, A. Petrou, G. Kioseoglou, I. Ozfidan, M. Korkusinski, P. Hawrylak, *Nature Nanotechnol.* **10**, 603 (2015).

[16] Y.J. Zhang, T. Oka, R. Suzuki, J.T. Ye, Y. Iwasa, *Science* **344**, 725 (2014).

[17] F. Withers, O. Del Pozo-Zamudio, S. Schwarz, S. Dufferwiel, P.M. Walker, T. Godde, A.P. Rooney, A. Gholinia, C.R. Woods, P. Blake, S.J. Haigh, K. Watanabe, T. Taniguchi, I.L. Aleiner, A.K. Geim, V.I. Falko, A.I. Tartakovskii, K.S. Novoselov, *Nano Lett.* **15**, 8223 (2015).

[18] K.F. Mak, K.L. He, J. Shan, T.F. Heinz, *Nature Nanotechnol.* **7**, 494 (2012).

[19] A.M. Jones, H. Yu, N.J. Ghimire, S. Wu, G. Aivazian, J.S. Ross, B. Zhao, J. Yan, D.G. Mandrus, D. Xiao, W. Yao, X. Xu, *Nature Nanotechnol.* **8**, 634 (2013).

[20] Q.H. Wang, K. Kalantar-Zadeh, A. Kis, J.N. Coleman, M.S. Strano, *Nature Nanotechnol.* **7**, 699 (2012).

[21] G. Wang, L. Bouet, D. Lagarde, M. Vidal, A. Balocchi, T. Amand, X. Marie, B. Urbaszek, *Phys. Rev. B* **90**, 075413 (2014).

[22] Z. Ye, T. Cao, K. O'Brien, H. Zhu, X. Yin, Y. Wang, S.G. Louie, X. Zhang, *Nature* **513**, 214 (2014).

[23] K. He, N. Kumar, L. Zhao, Z. Wang, K.F. Mak, H. Zhao, J. Shan, *Phys. Rev. Lett.* **113**, 026803 (2014).

[24] A. Chernikov, T.C. Berkelbach, H.M. Hill, A. Rigosi, Y. Li, O.B. Aslan, D.R. Reichman, M.S. Hybertsen, T.F. Heinz, *Phys. Rev. Lett.* **113**, 076802 (2014).

[25] G. Wang, E. Palleau, T. Amand, S. Tongay, X. Marie, B. Urbaszek, *Appl. Phys. Lett.* **106**, 112101 (2015).

[26] X.X. Zhang, Y. You, S.Y.F. Zhao, T.F. Heinz, *Phys. Rev. Lett.* **115**, 257403 (2015).

[27] G. Wang, L. Bouet, D. Lagarde, M. Vidal, A. Balocchi, T. Amand, X. Marie, B. Urbaszek, *Phys. Rev. B* **90**, 075413 (2014).

[28] A. Arora, M. Koperski, K. Nogajewski, J. Marcus, C. Faugeras, M. Potemski, *Nanoscale* **7**, 10421 (2015).

[29] J.S. Ross, S. Wu, H. Yu, N.J. Ghimire, A.M. Jones, G. Aivazian, J. Yan, D.G. Mandrus, D. Xiao, W. Yao, X. Xu, *Nature Commun.* **4**, 1 (2013).

[30] A.A. Mitioglu, P. Plochocka, J.N. Jadczak, W. Escoffier, G.L.J.A. Rikken, L. Kulyuk, D.K. Maude, *Phys. Rev. B* **88**, 245403 (2013).

[31] A. Singh, G. Moody, K. Tran, M.E. Scott, V. Overbeck, G. Berghäuser, J. Schaibley, E.J. Seifert, D. Pleskot, N.M. Gabor, J. Yan, D.G. Mandrus, M. Richter, E. Malic, X. Xu, X. Li, *Phys. Rev. B* **93**, 041401 (2016).

[32] T. Godde, D. Schmidt, J. Schmutzler, M. Aßmann, J. Debus, F. Withers, E.M. Alexeev, O. Del Pozo-Zamudio, O.V. Skrypka, K.S. Novoselov, M. Bayer, A.I. Tartakovskii, *Phys. Rev. B* **94**, 165301 (2016).

[33] P. Tonndorf, R. Schmidt, P. Böttger, X. Zhang, J. Börner, A. Liebig, M. Albrecht, C. Kloc, O. Gordan, D.R.T. Zahn, S. Michaelis de Vasconcellos, R. Bratschitsch, *Opt. Express* **21**, 4908 (2013).

[34] S.Y. Chen, C. Zheng, M.S. Fuhrer, J. Yan, *Nano Lett.* **15**, 2526 (2015).

[35] H. Sahin, S. Tongay, S. Horzum, W. Fan, J. Zhou, J. Li, J. Wu, F.M. Peeters, *Phys. Rev. B* **87**, 165409 (2013).

[36] J. Jadczak, D.O. Dumcenco, Y.S. Huang, Y.C. Lin, K. Suenaga, P.H. Wu, H.P. Hsu, K.K. Tiong, *J. Appl. Phys.* **116**, 193505 (2014).

[37] A.M. Jones, H. Yu, J.R. Schaibley, J. Yan, D.G. Mandrus, T. Taniguchi, K. Watanabe, H. Dery, W. Yao, X. Xu, *Nat. Phys.* **12**, 323 (2016).

[38] S. Tongay, J. Zhou, C. Ataca, J. Liu, J.S. Kang, T.S. Matthews, L. You, J. Li, J.C. Grossman, J. Wu, *Nano Lett.* **13**, 2831 (2013).

[39] B. Miller, E. Parzinger, A. Vernickel, A.W. Holleitner, U. Wurstbauer, *Appl. Phys. Lett.* **106**, 122103 (2015).

[40] S. Glasberg, G. Finkelstein, H. Shtrikman, I. Bar-Joseph, *Phys. Rev. B* **59**, 10425R (1999).

[41] J. Jadczak, L. Bryja, A. Wójs, M. Potemski, *Phys. Rev. B* **85**, 195108 (2012).

[42] G. Bartsch, M. Gerbracht, D.R. Yakovlev, J.H. Blokland, P.C.M. Christianen, E.A. Zhukov, A.B. Dzyubenko, G. Karczewski, T. Wojtowicz, J. Kossut, J.C. Maan, M. Bayer, *Phys. Rev. B* **83**, 235317 (2011).